Research Article

Influence of seed layer thickness on properties of electrodeposited ZnO nanostructured films

M. D. Reyes Tolosa[1] · M. Alajami[1] · A. E. Montero Reguera[2] · L. C. Damonte[3] · M. A. Hernández-Fenollosa[1]

Abstract
The quality and properties of electrodeposited nanostructured ZnO films are improved when they are deposited on a crystal lattice-matching substrate. To this end, a highly conductive indium tin oxide substrate is covered with an interlayer of ZnO using direct-current magnetron sputtering. In this manuscript, we describe the effect of this interlayer on the morphological and optical properties of several nanostructured ZnO films grown by different electrodeposition methods. The thickness of the ZnO interlayer was varied starting from ultrathin layers of 10 nm all the way up to 230 nm as determined by ellipsometry. The structural and optical properties of the nanostructured ZnO films deposited on top of these interlayers were characterized using field emission scanning electron microscopy (FESEM), atomic force microscopy and UV–visible spectroscopy. Optimum properties of the nanostructured ZnO films for application in thin-film optoelectronic devices are obtained when the ZnO interlayer has a thickness of approximately 45 nm. This is the case for all the electrodeposition methods used in this work.

Keywords ZnO films · Electrodeposition · DC magnetron sputtering · Optical properties · Nanostructures · Band gap energy

1 Introduction

Zinc oxide is a remarkable semiconductor with many applications due to its unique properties. It has a wide band gap with a direct energy gap, which is between 3.2 and 3.4 eV at room temperature, a large exciton binding energy of 60 meV, a high transparency and a low electrical resistivity [1, 2]. It is nontoxic and easily fabricated [3], resulting in a potentially lower cost for ZnO-based devices [4] such as solar cells [5, 6], photoconductors [7, 8] and gas sensors [9], to name a few. The efficiency and performance of these optoelectronic devices are largely dependent on the optical and electrical properties of ZnO film. There are numerous methods to grow ZnO thin films, such as spray pyrolysis [10, 11], vapor–liquid–solid processes [12], sol–gel [13, 14], electrodeposition (ED) [15, 16] and different forms of vapor phase deposition, using a pulsed laser [17] or ion-assisted sputtering [18–20]. Among these methods, ED is a low-cost alternative that offers a high degree of control over the film morphology, such as nanostructures, through optimization of the deposition parameters. Transparent conductive oxide-coated glass substrates are essential for optoelectronic devices as they allow light to enter/escape from an optoelectronic device while applying an electrical potential. Indium tin oxide (ITO)-coated glass substrates are by far the most used example. During the preparation of optoelectronic devices, layers are deposited sequentially on a substrate, and to obtain a good morphology of the electrodeposited ZnO layer, a good lattice match between ZnO nanostructures and the

✉ M. A. Hernández-Fenollosa, mhernan@fis.upv.es | [1]Instituto de Tecnología de Materiales, Universitat Politècnica de Valencia, Camino de Vera s/n, 46022 Valencia, Spain. [2]Departamento de Termodinámica Aplicada, Universitat Politècnica de Valencia, Camino de Vera s/n, 46022 Valencia, Spain. [3]Departamento de Física, Facultad de Ciencias Exactas, CCT, CONICET, Universidad Nacional de La Plata-IFLP, C.C. 67, 1900 La Plata, Argentina.

SN Applied Sciences (2019) 1:1245 | https://doi.org/10.1007/s42452-019-1293-7

Received: 1 July 2019 / Accepted: 16 September 2019 / Published online: 20 September 2019

substrate is required. When such nanostructured thin films are deposited directly onto ITO-coated glass, they have a wide distribution of grain sizes, high defect concentrations and poor optical performances [21]. These poor properties of the nanostructured ZnO layer are a result of the different crystal lattices of the substrate and the top layer. Thus, if an intermediate layer is introduced in between the nanostructured ZnO layer and the substrate, the structure of the top film can be better controlled. This is important as it has been shown that surface orientation and termination have a large effect on the work function of these films and as a consequence also on the overall properties of the devices employing these films [22–26]. The interlayer provides the nucleation centers for the subsequent ED film growth, improving the uniformity of ZnO nanostructures [27]. In a previous work from our team, the first relation between the interlayer growth conditions and the properties of nanostructured ZnO films was described [28].

In this work, we studied the influence of ZnO interlayer thickness on the structural and optical properties of ED-grown ZnO films. We have used a two-step deposition procedure, in which a ZnO interlayer is first deposited onto the substrate by direct-current (DC) magnetron sputtering, considered to be a suitable technique due to the inherent ease with which the deposition parameters can be controlled. Moreover, it can deposit large-area films and the growth rate is low enough to generate ultrathin multicrystalline films even on nonlattice-matched substrates [29]. It is complementary to ED film growth as the latter allows for a much large control over the film nanostructure and subsequently its properties. A schematic illustration of the deposition process of the different thin ZnO layers is shown in Fig. 1. Previous research has discussed the interlayer thickness dependence on structural, electrical and optical properties of ZnO nanorod-based films, deposited using radio-frequency (RF) magnetron sputtering [30, 31] and hydrothermal methods [32].

We varied the ZnO interlayer thicknesses starting from ultrathin layers of 10 nm all the way up to 230 nm to determine the optimum interlayer thickness that leads to films with the structural and optical properties needed for optoelectronic devices. To this end, the ED film growth conditions were also varied, taking into account previous studies on different ED procedures for nucleation and growth [33–35]. Potentiostatic, galvanostatic, pulsed-current and pulsed-potential electrochemical deposition methods were applied on previously sputtered interlayers, to analyze the influence on the morphological uniformity of the nanostructured ZnO film and on the final properties of the complete assembly. We find that interlayers with a thickness between 20 and 45 nm lead to homogenous nanostructured ZnO films with optimum morphological and optical properties. Interlayers with thicknesses below 20 nm lead to regions of uncoated surface, whereas when the interlayer thickness exceeds 50 nm the absorption losses become excessive. This relationship is independent of the type of ED method employed, confirming the importance of the interlayer on the final electrodeposited film properties.

2 Experimental

The ZnO thin films were fabricated on commercial glass slides covered with an ITO conductive layer from Asahi Glass Company (sheet resistance at room temperature 15 Ω/sq). Substrates were cleaned with soap and rinsed with deionized water, followed by sonication for 10 min in iso-propanol, after which they were dried carefully using nitrogen gas.

The ZnO films were studied with the following techniques: Ellipsometry (GES5E variable-angle spectroscopic ellipsometer) was used to measure the thickness of the ZnO interlayers. Atomic force microscopy (AFM, Veeco Multimode) was used to observe the surface morphologies of ZnO interlayers and surface roughness. Field emission scanning electron microscopy (FESEM, ULTRA 55 from Zeiss) was used to characterize the morphology of ZnO electrodeposited nanostructures. The absorption spectra for all obtained films were analyzed using a Newport UV–vis spectrophotometer in the 300–850 nm wavelength range at room temperature. Optical transmission spectra (Hamamatsu model L2175 150w Xe source spectrum) were recorded, and the absorption coefficient (α) for all studied thicknesses was calculated.

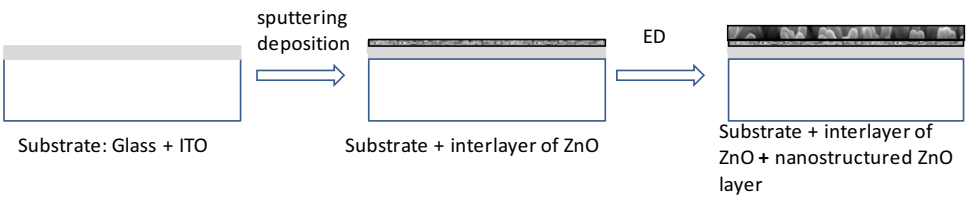

Fig. 1 Schematic illustration of the deposition process of the different thin ZnO layers

2.1 Sputtered ZnO deposition procedures (interlayer of ZnO)

ITO-covered substrates were placed in a homemade DC sputtering chamber. The cathode used was ZnO with purity of 99.999%, and the working parameters were as follows: magnetron plasma at 100 W, Ar pressure of 0.2 mbar and substrate temperature of 300 °C. Only the deposition time was varied (3, 4, 5, 6, 7, 8, 10, 20, 30, 60, 90, 120 min) with the purpose of obtaining different thicknesses.

2.2 Electrodeposited ZnO growth procedures (nanostructured ZnO film)

Nanostructured thin films were grown by electrodeposition in a three-electrode electrochemical cell. The aqueous electrolyte was composed of $ZnCl_2$ (5×10^{-3} M), KCl (0.1 M) and saturated with dissolved oxygen maintained with constant pure oxygen gas flow (bubbling). The process was held at a constant temperature of 70 °C. To control the electrical parameters that manage the growth, we used an Autolab PGSTAT302 N potentiostat (Metrohm, Utrecht, the Netherlands) with an ADC 10 M card for ultrafast measurement acquisition (one sample every 10 ns).

3 Results

One of the main uncertainties we wish to address is which ZnO interlayer thickness leads to the best nanostructured ZnO film, when considering homogeneity and optical properties. To do this, we first prepared a series of sputtered ZnO interlayers with increasing thickness on top of ITO-coated glass substrates. Their thickness increases with increasing deposition time of the sputtering process as determined by ellipsometry and depicted in Table 1 and Fig. 2. For each sputtered ZnO thickness, an average of five samples was prepared and the average surface roughness (ASR) was determined via AFM. The data points obtained are depicted in Table 1, and for clarity compiled graphically in Fig. 2.

From the data shown in Fig. 2, one can clearly observe the linear relation between the deposition time and the film thickness. This is expected and confirms the proper functioning of the tool and continuous deposition of the ZnO. The relation between the ASR and the sputtering time is less direct as the spreading in data points is rather large, particularly for short deposition times. To understand the reason for this spreading, the AFM images of the different ZnO interlayers are insightful (Fig. 3). There we observe that the density of particles in the interlayer increases as sputtering time progresses. For ultrathin layers (less than 20 nm), we can note that the surface is not covered homogenously with the sputtered material, and the surface roughness appears to be independent of layer thickness. Hence, for these very thin ZnO interlayers, the surface roughness merely indicates the presence of uncoated substrate among ZnO layers and as such it does not describe the surface roughness of the ZnO films. However, the grain shape and size change with the film thickness: The large grains present in the thicker films are formed by smaller ones. Samples with a thickness of around 11 nm show surfaces of ZnO films that have an island-like nonuniform grain size. From 11 to 20 nm, we have found homogeneous areas which are covered by small-sized grains. The grains become more uniform as the film thickness increases. After a certain thickness, approximately 20 nm, the surface roughness increases with the increasing thickness of ZnO films because of the increasing grain size [36]. It is not trivial to extract accurate grain dimensions from the films with a thickness below 40 nm; however, these grains all have diameters below 60 nm. With thicker films, it becomes easier to obtain grain size information and these increase to diameters of 150 nm for films with thicknesses in the range of 120 nm to over 300 nm for the grains of the thickest films.

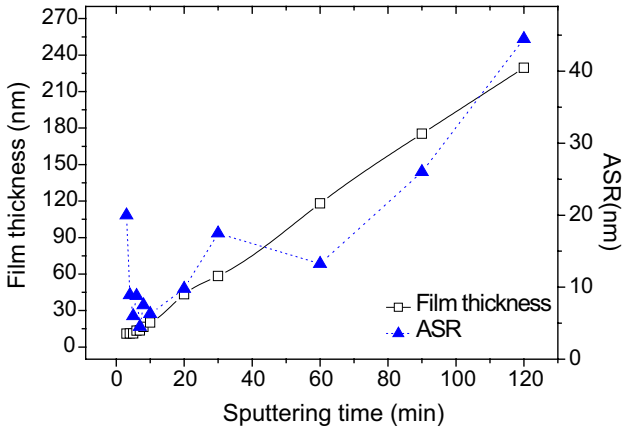

Fig. 2 Relation between ZnO interlayer thickness (open squares) and average surface roughness (ASR) (blue filled triangles) on deposition time

Table 1 Variation in film thickness and average surface roughness (ASR) for ZnO films with different sputtering times

Sputtering time (min)	3	4	5	6	7	8	10	20	30	60	90	120
Film thickness (nm)	10.96	11.08	11.15	13.36	13.64	16.5	20.13	43.32	58.33	118.1	175.4	229.5
ASR (nm)	20	8.9	6	8.8	4.5	7.5	6.3	9.8	17.5	13.25	26	44.5

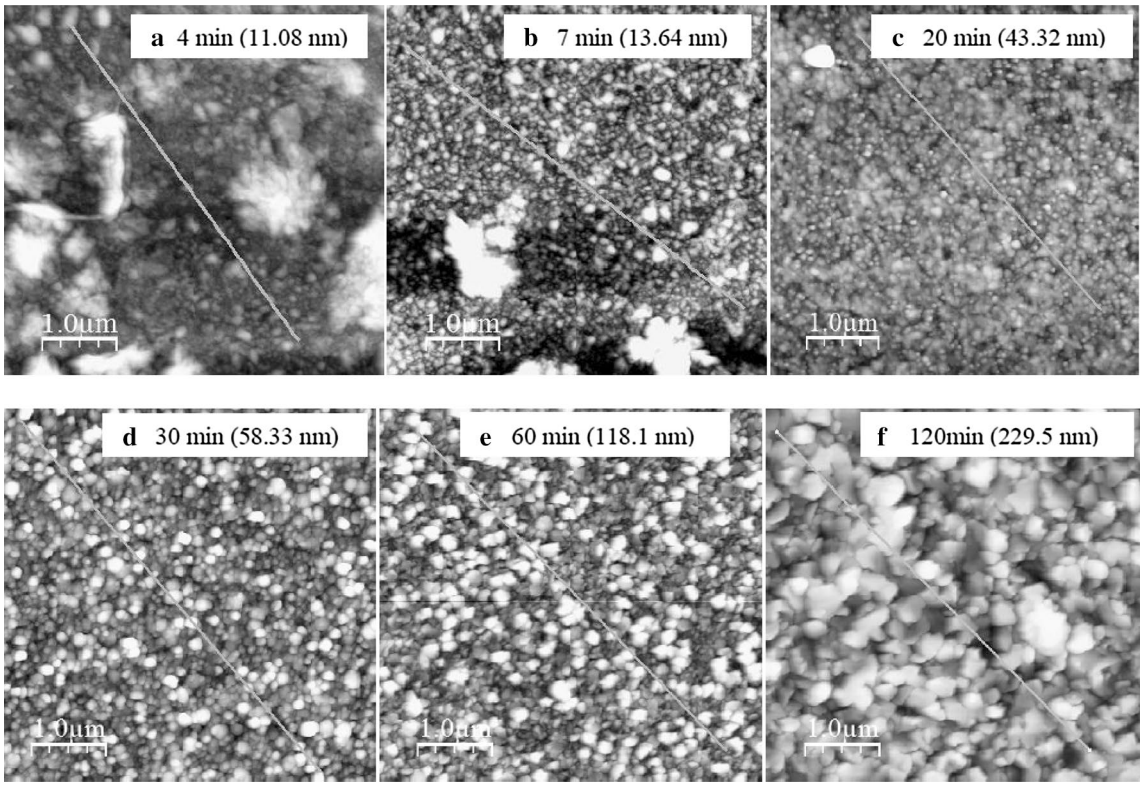

Fig. 3 AFM images of ZnO interlayers as a function of deposition time in minutes

The growth of the particles leads to the formation of mound-like structures which continue to grow in three dimensions once the surface is completely covered. Due to the growth of these structures in three dimensions, the grain size increases and therefore the ASR increases with increasing deposition time (and increasing ZnO film thickness).

Now that a relation between the surface structure, ASR and thickness of the interlayer has been established, it is possible to study their influence on the morphology of the ZnO nanostructures. Four different electrodeposition methods were used initially, only on ITO-covered substrates consisting of a sputtered ZnO interlayer with a thickness of 43 nm: (1) potentiostatically for 10 min; (2) galvanostatically for 10 min; (3) pulsed potential at a frequency of 0.5 Hz for 20 min; and (4) pulsed current at a frequency of 0.5 Hz for 20 min. All the experimental details implemented to develop these ED growth methods can be consulted in our previous works [34, 35].

Figure 4 shows FESEM images of the surface of the nanostructured ZnO layers with the four different methods as described above. In Fig. 4a, b, the images of the ZnO deposited with a fixed potential and current are displayed, respectively. Under these growth conditions, the nanostructures of ZnO form an array of nanorods with diameters of around 100 nm. However, when a pulsed process is used, hexagonal nanoplates with a diameter of 200 nm are formed (Fig. 4c and d). In all four ED methods, however, the ZnO shows a nanostructured morphology that will induce the so-called moth eye effect [37, 38] that will induce light trapping, which is beneficial for use in optoelectronic devices, such as solar cells [39].

Hence, since we have established that all four ED methods lead to nanostructured morphologies, in the following we focus on the potentiostatic ED method to study the effect of the ZnO interlayer thickness on the nanostructured ZnO properties.

Figure 5 shows FESEM images of the surface of nanostructured ZnO layers deposited potentiostatically on substrates (ITO and glass) that contain sputtered ZnO interlayers with different thicknesses. In Fig. 5a and b, one can observe that the surface of the sample is not fully covered by the electrodeposited layer. This is most likely due to incomplete coverage of the ZnO interlayer due to insufficient sputtering time as discussed above. For the substrates that contain interlayer thicknesses above 40 nm, a completely covered ZnO nanostructured surface is obtained (Fig. 5c and d). Additionally, as the interlayer thickness increases, the diameter of the nanostructures increases and their density decreases. As seen in Fig. 3, grain and particle size increase with increasing interlayer thickness, and since the interlayer serves as a template for

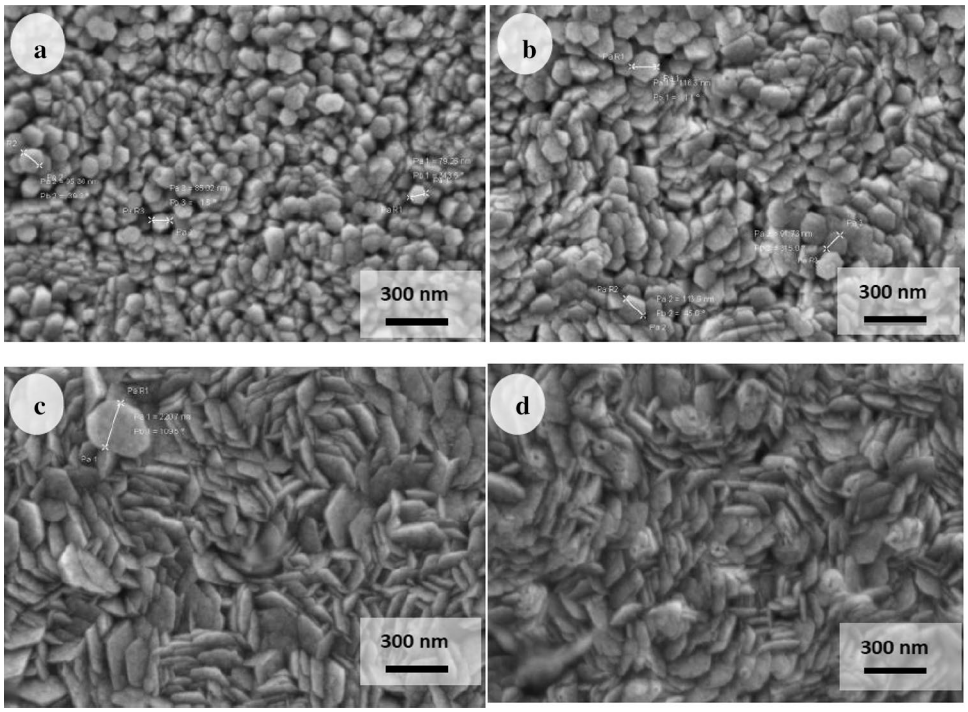

Fig. 4 FESEM images of nanostructured ZnO films deposited with different types of electrodeposition onto ZnO interlayers with a thickness of 43.8 nm: **a** potentiostatically, **b** galvanostatically, **c** pulsed potential and **d** pulsed current

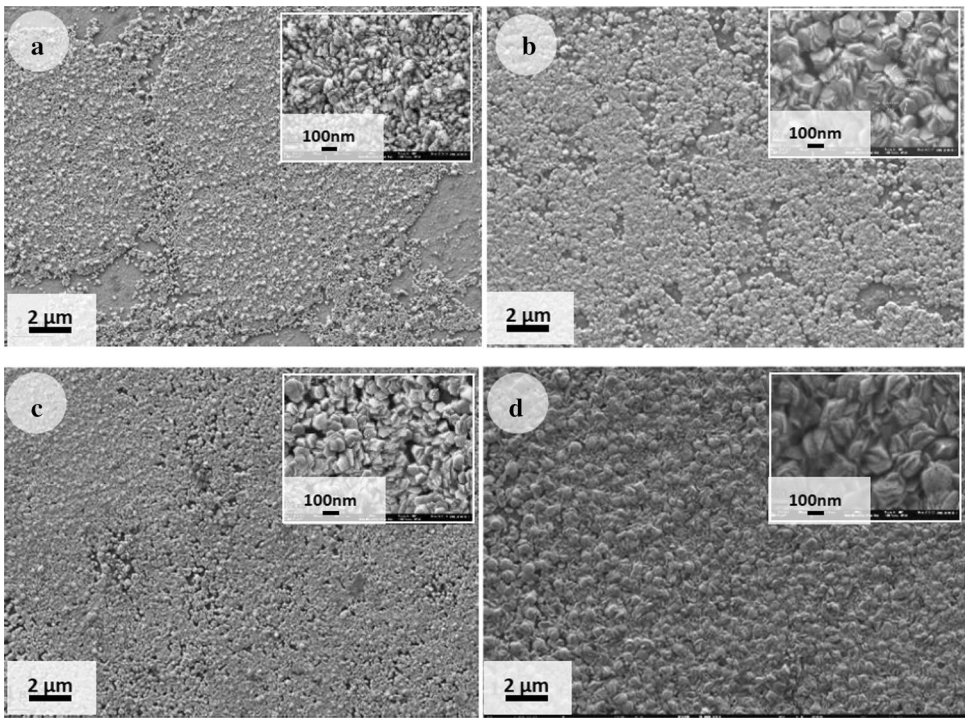

Fig. 5 FESEM images of nanostructured ZnO films deposited potentiostatically onto ZnO interlayers with thicknesses of: **a** 13.6 nm, **b** 20.1 nm, **c** 43.3 nm and **d** 58.3 nm

the nanostructures, the diameter of the nanostructures also increases.

The optical transmittances of the sputtered ZnO films are shown in Fig. 6 as a function of their thickness. The average transmittance in the visible range is found to be greater than 85% for all the samples, and for thicknesses larger than 20 nm, we notice a gradual UV shielding effect. This characteristic is in agreement with the fact that ZnO is a direct band-gap semiconductor with an energy gap between 3.2 and 3.4 eV.

The transmission spectra of the nanostructured ZnO films electrodeposited onto sputtered ZnO interlayers with a thickness of 43.32 nm using four different methods are shown in Fig. 7. The transmittance of the nanostructured

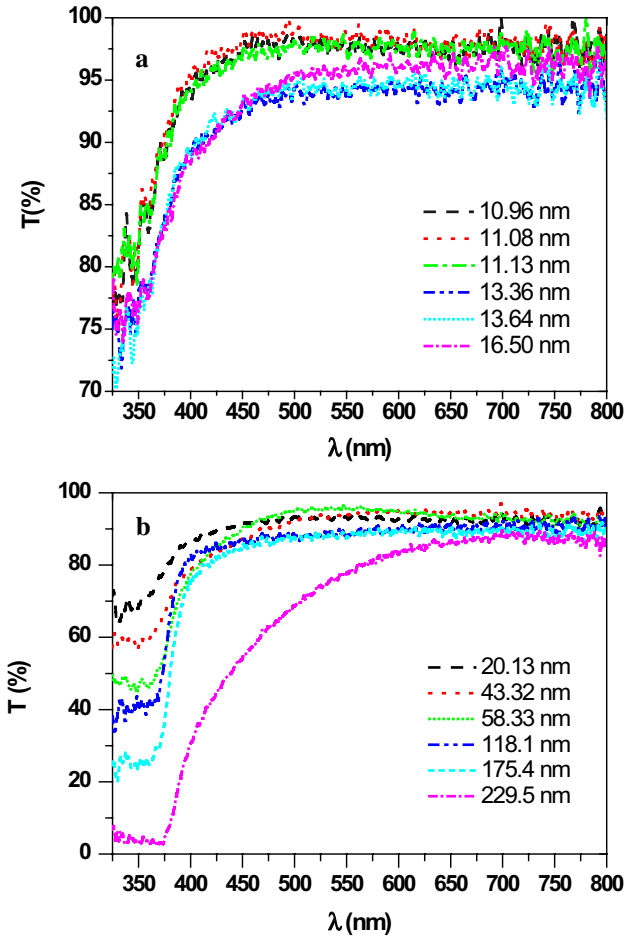

Fig. 6 Transmission spectra of ZnO interlayers with different thicknesses; **a** ultrathin layers (thickness < 20 nm) and **b** thin layers (thickness > 20 nm)

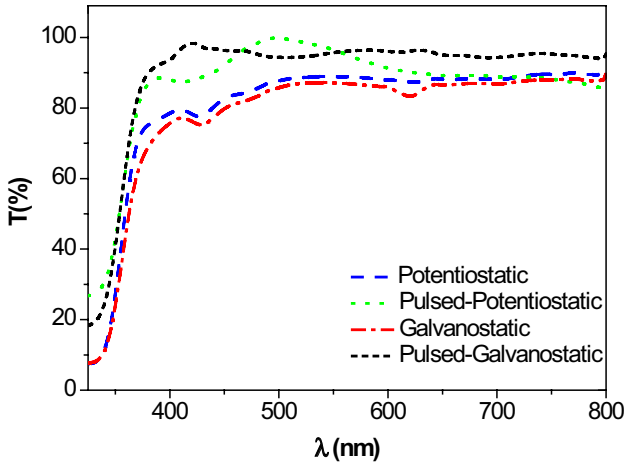

Fig. 7 Transmission spectra of nanostructured ZnO films deposited with different electrodeposition methods: potentiostatically, galvanostatically, pulsed-potential and pulsed-current processes

ZnO films deposited using pulsed-potential and pulsed-current methods is significantly higher than that of the films prepared by static voltage and current growth conditions. The samples grown in pulsed conditions present nanostructures of larger diameter, which entails a decrease in the number of light scattering centers and therefore a higher transmittance.

In Fig. 8, we depict the transmission spectra of nanostructured ZnO films deposited onto the interlayer with different thicknesses. The sample deposited onto 43.32 nm shows the highest transmission of light in the visible range, while the samples on 13.64 and 20.13 nm interlayer thickness absorb more light due to the inhomogeneous interlayer. The sample with seed layer of 58.33 nm shows about 70% transmission.

In general, the sputtered material is highly transparent compared to the electrodeposited material, which is white/opaque in appearance. From Figs. 7 and 8, we see that sputtered and nanostructured ZnO films transmit around 95% and 85% of incident photons, respectively, for wavelengths greater than 600 nm when the interlayer thickness remains below 43 nm approximately. The difference in transmission is attributed to thickness, surface roughness and scattering centers. The milky appearance of nanostructured ZnO layers is mainly due to the diffusion of light due to the roughness of the layers, although inclusions of $Zn(OH)_2$ during electrodeposition from aqueous solution could also contribute to this appearance [40]. For electrodeposited layers, when the electrodeposition techniques were varied (Figs. 4 and 7), we can note that the morphologies of the potentiostatic and galvanostatic nonpulsed depositions somewhat resemble each other, with comparable nanostructure diameters, explaining the similarity in transmission spectra; the same phenomenon was observed with pulsed electrodepositions.

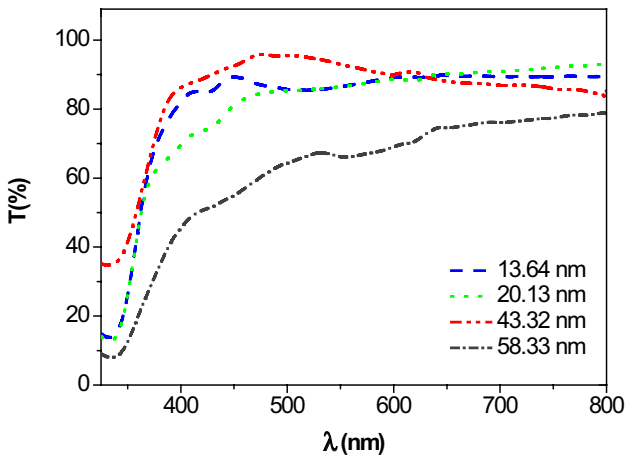

Fig. 8 Transmission spectra of potentiostatically deposited nanostructured ZnO films as a function of interlayer thickness

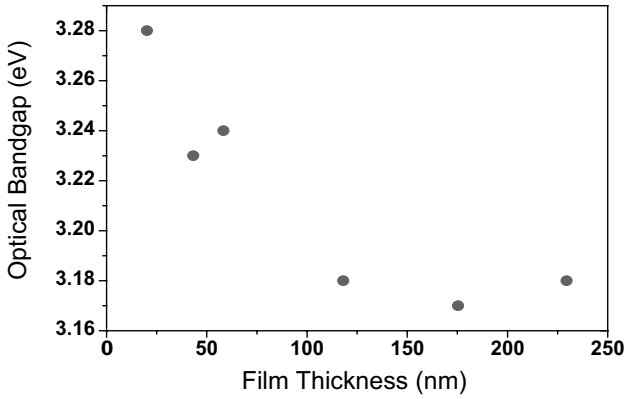

Fig. 9 Optical energy gap (E_g) versus film thickness of the sputtered ZnO films

While varying the interlayer thicknesses (Fig. 5 and Fig. 8), we can see that ZnO interlayers greater than 50 nm have significantly lower transmission of light than thinner ZnO interlayers. Taking into account the inhomogeneous layer of nanostructured ZnO on interlayers of 20 nm or less, it can be concluded that the more suitable interlayer thicknesses are those in between 20 and 50 nm. In this range, the ZnO interlayer covers the substrate homogeneously, but is not so thick that it hinders the transmission of light. According to our study, the optimal thickness is around 45 nm.

The effect of thickness on the optical band gap of ZnO sputtered films has been determined from the transmittance data. The absorption coefficient (α) is calculated using the Beer–Lambert relation. The relationship between the absorption coefficient and the incident photon energy (hυ) is given by the following equation [41]:

$$(\alpha h\nu)^2 = A(h\nu - E_g)$$

where A is a constant and E_g is the optical band gap. The E_g can be determined by extrapolating the linear regions of $(\alpha h\upsilon)^2$ to zero absorption. From this equation, we calculate the E_g for the sputtered films and the results are shown in Fig. 9. The band gap of the films varied between 3.17 to 3.28 eV, and the band gap decreases with increased film thickness, showing the n-type nature of the ZnO semiconductor. This decrease in band gap may be attributed to the presence of unstructured defects which increase the density of localized states in the band gap and consequently decrease the energy gap [42]. We also found variations in crystallite size (which are below 60 nm for samples with thicknesses less than 40 nm, as we have appointed previously from the AFM images of ZnO interlayers) that can induce such changes [1, 43].

According to the literature, the oxygen and Zn vacancies as well as Zn interstitials seem to be the predominant ionic defects and the growth environment controls their concentration in ZnO films. These defects introduce the levels in the band gap of the semiconductor, responsible for transitions between different charge states and the shift of the optical band gap to values smaller than the bulk $E_g \sim 3.3$ eV [44].

4 Conclusions

Two growth methods of ZnO thin film have been performed in this work to study the properties of nanostructured ZnO layers. First, ZnO thin films were sputtered on conductive glass substrate, acting as an interlayer, and electrodeposited ZnO (nanostructured ZnO) thin films were subsequently grown on the sputtered film. The properties of the nanostructured ZnO layers depend strongly on the interlayer morphology, which is controlled mainly by its thickness. From the FESEM images, we can note that the size of the electrodeposited ZnO nanostructures increases and the density per unit area decreases with increasing interlayer thickness. In the case of ultrathin interlayers (less than 20 nm), this layer was not continuous or homogeneous, and consequently the sample is not completely covered when the nanostructured layer is deposited. On the other hand, samples with interlayers greater than 50 nm show a significant drop in light transmission.

Therefore, with this study we have verified that an interlayer thickness of around 45 nm is a crucial factor for formation of uniform nanostructured ZnO thin film. This thickness is crucial to preserve the high transmission of the nanostructured ZnO layer in the visible range and is enough to be continuous and homogeneous and thereby ensure better morphological characteristics of the electrodeposited layer. These properties make the nanostructured ZnO layer suitable in many applications such as transparent electrodes of thin film solar cells, transparent oxide thin-film transistors or light-emitting diodes.

Acknowledgements We thank Prof. A. Segura of the Universitat de València for the facilities with the sputtering equipment.

Compliance with ethical standards

Conflict of interest The authors declare that they have no conflict of interest.

References

1. Marotti RE, Giorgi P, Machado G, Dalchiele EA (2006) Crystallite size dependence of band gap energy for electrodeposited ZnO grown at different temperatures. Sol Energy Mater Sol Cells 90:2356–2361

2. Marotti RE, Guerra DN, Bello C, Machado G (2004) Bandgap energy tuning of electrochemically grown ZnO thin films by thickness and electrodeposition potential. Sol Energy Mater Sol Cells 82:85–103
3. Jin ZC, Hamberg I, Grangvist CG (1988) Optical properties of sputter-deposited ZnO: Al thin films. J Appl Phys 64:5117–5131
4. Chopra KL, Major S, Pandya DK (1983) Transparent conductors—a status review. Thin Solid Films 102:1–46
5. Kiliç B, Wang L, Ozdemir O, Lu M, Tüzemen S (2013) One-dimensional (1D) ZnO nanowires dye sensitized solar cell. J Nanosci Nanotechnol 13:333–338
6. Granqvist CG (2007) Transparent conductors as solar energy materials: a panoramic review. Sol Energy Mater Sol Cells 9:1529–1598
7. Mallampati B, Nair SV, Ruda HE, Philipose U (2015) ZnO nanowire based photoconductor with high photoconductive gain. Mater Res Soc Symp Proc 1805:720–726
8. Benlamri M, Bothe KM, Ma AM, Shoute G, Afshar A, Sharma H, Mohammadpour A, Gupta M, Cadien KC, Tsui YY, Shankar K, Barlage DW (2014) High-mobility solution-processed zinc oxide thin films on silicon nitride. Phys Status Solidi RRL 8:871–875
9. Galstyan V, Comini E, Ponzoni A, Sberveglieri V, Sberveglieri G (2016) ZnO quasi-1D nanostructures: synthesis, modeling, and properties for applications in conductometric. Chem Sens 4:6–27
10. Ayouchi R, Leinen D, Martin F, Gabas M, Dalchiele E, Ramos-Barrado JR (2003) Preparation and characterization of transparent ZnO thin films obtained by spray pyrolysis. Thin Solid Films 426:68–77
11. Rahmane S, Aida MS, Chala A, Temam HB, Djouadi MA (2007) Elaboration of transparent undoped ZnO and Al-doped ZnO thin films by spray pyrolysis and their properties. Plasma Process Polym 4:356–358
12. Zhu G, Zhou Y, Wang S, Yang R, Ding Y, Wang X, Bando Y, Wang ZL (2012) Synthesis of vertically aligned ultra-long ZnO nanowires on heterogeneous substrates with catalyst at the root. Nanotechnology 23:055604–055610
13. Hossein A, Kar P, Farsinezhad S, Sharma H, Shankar K (2015) Effect of sol stabilizer on the structure and electronic properties of solution-processed ZnO thin films. RSC Adv 5:87007–87018
14. Majumder SB, Jain M, Dobal PS, Katiyar RS (2003) Investigations on solution derived aluminium doped zinc oxide thin films. Mater Sci Eng 103:16–25
15. Gao XD, Peng F, Li XM, Yu WD, Qiu JJ (2007) Growth of highly oriented ZnO films by the two-step electrodeposition technique. J Mater Sci 42:9638–9644
16. Dalchiele EA, Giorgi P, Marotti RE, Martín F, Ramos-Barrado JR, Ayouci R, Leinen D (2001) Electrodeposition of ZnO Thin Films on n-Si (100). Sol Energy Mater Sol Cells 70:245–254
17. Craciun V, Elders J, Gardeniev JGE, Boyd IW (1994) Characteristics of high quality ZnO thin films deposited by pulsed laser deposition. Appl Phys Lett 65:2963–2965
18. Bang KH, Hwang DK, Myoung JM (2003) Effects of ZnO buffer layer thickness on properties of ZnO thin films deposited by radio-frequency magnetron sputtering. Appl Surf Sci 207:359–364
19. Hayashi Y, Kondo K, Murai K, Moriga T, Nakabayashi I, Fukumoto H, Tominag K (2004) ZnO–SnO_2 transparent conductive films deposited by opposed target sputtering system of ZnO and SnO_2 targets. Vacuum 74:607–611
20. Minami T, Nanto H, Takata S (1983) UV emission from sputtered zinc oxide thin films. Thin Solid Films 109:379–384
21. Gu CD, Li J, Lian JS, Zheng GQ (2007) Electrochemical synthesis and optical properties of ZnO thin film on In_2O_3: Sn (ITO)-coated glass. Appl Surf Sci 253:7011–7015
22. Korber C, Suffner J, Klein A (2010) Surface energy controlled preferential orientation of thin films. J Phys D Appl Phys 43:055301–055304
23. Dadgour HF, Endo K, De VK, Banerjee K (2010) Grain-orientation induced work function variation in nanoscale metal-gate transistors; part I: modeling, analysis, and experimental validation. IEEE Trans Electron Devices 57:2504–2514
24. Sadewasser S, Glatzel T, Schuler S, Nishiwaki S, Kaigawa R, Lux-Steiner MC (2003) Kelvin probe force microscopy for the nano scale characterization of chalcopyrite solar cell materials and devices. Thin Solid Films 257:431–432
25. Boubenia S, Dahiya AS, Poulin-Vittrant G, Morini F, Nadaud K, Alquier DA (2017) Facile hydrothermal approach for the density tunable growth of ZnO nanowires and their electrical characterizations. Sci Rep 7:15187–15196
26. Ghayour H, Rezaie HR, Mirdamadi S, Nourbakhsh AA (2011) The effect of seed layer thickness on alignment and morphology of ZnO nanorods. Vacuum 86:101–105
27. Bae YS, Kim DC, Ahn CH, Kim JH, Cho HK (2010) Growth of ZnO nanorod arrays by hydrothermal method using homo-seed layers annealed at various temperatures. Surf Interface Anal 42:978–982
28. Donderis V, Hernández-Fenollosa MA, Damonte LC, Marí B, Cembrero J (2007) Enhancement of surface morphology and optical properties of nanocolumnar ZnO films. Superlattices Microstruct 42:461–467
29. Chichibu SF, Yoshida T, Onuma T, Nakanishi H (2002) Helicon-wave-excited-plasma sputtering epitaxy of ZnO on sapphire (0001) substrates. J Appl Phys 91:874–877
30. Bouderbala M, Hamzaoui S, Amrani B, Reshak AH, Adnane M, Sahraoui T, Zerdali M (2008) Thickness dependence of structural, electrical and optical behaviour of undoped ZnO thin films. Phys B 403:3326–3330
31. Kishimoto S, Yamamoto T, Nakagawa Y, Ikeda K, Makino H, Yamada T (2006) Dependence of electrical and structural properties on film thickness of undoped ZnO thin films prepared by plasma-assisted electron beam deposition. Superlattices Microstruct 39:306–313
32. Suchea M, Christoulakis S, Katharakis M, Vidakis N, Koudoumas E (2009) Influence of thickness and growth temperature on the optical and electrical properties of ZnO thin films. Thin Solid Films 517:4303–4306
33. Mridha S, Basak D (2007) Effect of thickness on the structural, electrical and optical properties of ZnO films. Mater Res Bull 42:875–882
34. Reyes Tolosa MD, Orozco-Messana J, Lima ANC, Camaratta R, Pascual M, Hernandez-Fenollosa MA (2011) Electrochemical deposition mechanism for ZnO nanorods: diffusion coefficient and growth models. J Electrochem Soc 158:107–110
35. Reyes Tolosa MD, Orozco-Messana J, Damonte LC, Hernandez-Fenollosa MA (2011) ZnO nanoestructured layers processing with morphology control by pulsed electrodeposition. J Electrochem Soc 158:452–455
36. Laukaitis G, Lindroos S, Tamulevicius S, Leskela M (2001) Stress and morphological development of CdS and ZnS thin films during the SILAR growth on (1 0 0) GaAs. Appl Surf Sci 185:134–139
37. Ludwig W, Ohm W, Correa-Hoyos JM, Zhao Y, Lux-Steiner MC, Gledhill S (2013) Electrodeposition parameters for ZnO nanorod arrays for photovoltaic applications. Phys Status Solidi A 210:1557–1563
38. Chopra KL, Das SR (1983) Thin film solar cells. Springer, New York
39. Ohm W, Riedel W, Askünger Ü, Heinemann MD, Kaufmann CA, Lopez Garcia J, Izquierdo V, Fontané X, Goislard T, Lux-Steiner MC, Gledhill S (2015) An overview of technological aspects of Cu(In, Ga)Se_2 solar cell architectures incorporating ZnO nanorod arrays. Phys Status Solidi A 212:76–87

40. Wang Q, Wang G, Jie J, Han X, Xu B, Hou JG (2005) Annealing effect on optical properties of ZnO films fabricated by cathodic electrodeposition described. Thin Solid Films 492:61–65
41. Tao Y, Fu M, Zhao A, He D, Wang Y (2010) The effect of seed layer on morphology of ZnO nanorod arrays grown by hydrothermal method. J Alloys Compd 489:99–102
42. El-Zahed H, El- Korashy A, Abdel Rahman M (2003) Effect of heat treatment on some of the optical parameters of $Cu_9Ge_{11}Te_{80}$ films. Vacuum 68:19–27
43. Kumar M, Sasikumar C (2014) Electrodeposition of nanostructured ZnO thin film. Am J Mater Sci Eng 23:18–23
44. Wang J, Chen R, Xiang L, Komarneni S (2018) Synthesis, properties and applications of ZnO nanomaterials with oxygen vacancies: a review. Ceram Int 44:7357–7377